

# Analytical Methods

Accepted Manuscript



This is an *Accepted Manuscript*, which has been through the Royal Society of Chemistry peer review process and has been accepted for publication.

*Accepted Manuscripts* are published online shortly after acceptance, before technical editing, formatting and proof reading. Using this free service, authors can make their results available to the community, in citable form, before we publish the edited article. We will replace this *Accepted Manuscript* with the edited and formatted *Advance Article* as soon as it is available.

You can find more information about *Accepted Manuscripts* in the [Information for Authors](#).

Please note that technical editing may introduce minor changes to the text and/or graphics, which may alter content. The journal's standard [Terms & Conditions](#) and the [Ethical guidelines](#) still apply. In no event shall the Royal Society of Chemistry be held responsible for any errors or omissions in this *Accepted Manuscript* or any consequences arising from the use of any information it contains.

1

2  
3 **A low-cost microcontrolled photometer with one color**  
4 **recognition sensor for selective detection of Pb<sup>2+</sup> using gold**  
5 **nanoparticles**  
6  
7  
8

9  
10 Camilo de L. M. de Moraes<sup>1</sup>, Julyana C. Carvalho<sup>1,2</sup>, Celso Sant'Anna<sup>3</sup>, Mateus  
11 Eugênio<sup>3</sup>, Luiz H. S. Gasparotto<sup>1</sup>, Kássio M.G. Lima<sup>\*1</sup>  
12  
13

14  
15 <sup>1</sup>*Institute of Chemistry, Biological Chemistry and Chemometrics, Federal University*  
16 *of Rio Grande do Norte, Natal 59072-970, RN-Brazil*

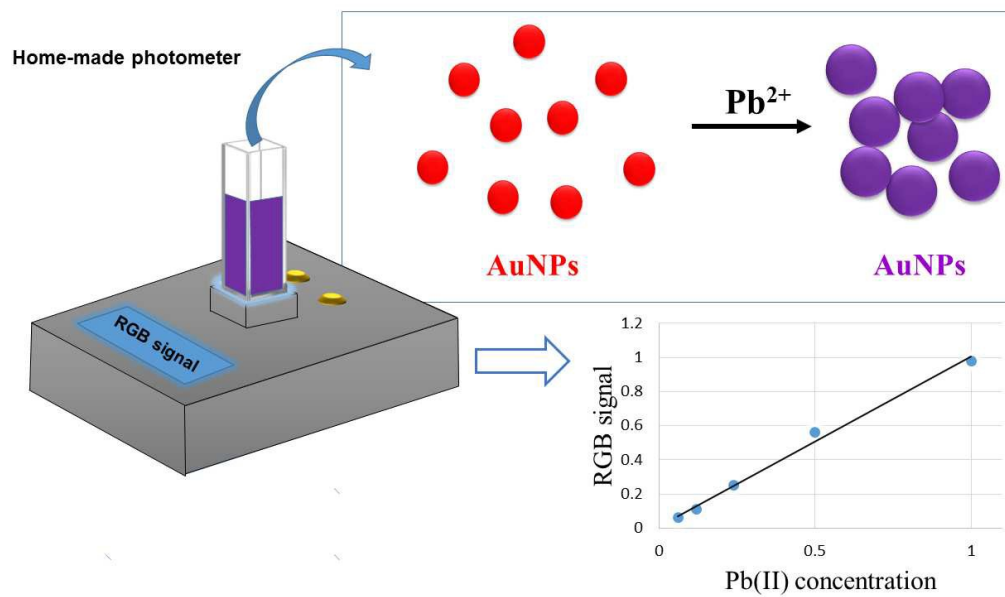
17 <sup>2</sup>*Federal Institute for Education, Science and Technology of Rio Grande do Norte,*  
18 *Natal 59015-000, RN-Brazil*

19 <sup>3</sup>*Laboratory of Biotechnology – Labio, National Institute of Metrology, Quality and*  
20 *technology – Inmetro, Duque de Caxias 25250-020, RJ-Brazil*  
21  
22  
23  
24  
25  
26  
27

28 **\* Correspondence to:** Prof. Dr. Kássio M.G. Lima, Institute of Chemistry, Biological  
29 Chemistry and Chemometrics, UFRN, Natal, 59072-970, Brazil; Email:  
30 kassiolima@gmail.com; Tel.: +55(84)3342 2323  
31  
32  
33  
34  
35  
36  
37  
38  
39  
40  
41  
42  
43  
44  
45  
46  
47  
48  
49  
50  
51  
52  
53  
54  
55  
56  
57  
58  
59  
60

2

ToC

1  
2  
3  
4  
5  
6  
7  
8  
9  
10  
11  
12  
13  
14  
15  
16  
17  
18  
19  
20  
21  
22  
23  
24  
25  
26  
27  
28  
29  
30  
31  
32  
33  
34  
35  
36  
37  
38  
39  
40  
41  
42  
43  
44  
45  
46  
47  
48  
49  
50  
51  
52  
53  
54  
55  
56  
57  
58  
59  
60

3

**Abstract:** The present work describes a microcontrolled photometer based on light-emitting-diodes (LED) for detection of  $\text{Pb}^{2+}$  using gold nanoparticles (AuNPs). The photometer makes use of a single LED as a light source, a sensor TCS230 (TAOS, USA) and an Arduino electronic card as acquisition system. On the sensor, the light from the three closely-adjointed red, green, and blue LED composing the “white” light source LED is contact-coupled to the map-illumination pointed toward the detection cell. To maintain a constant light intensity - a common white-color LED (emitting a 450–620 nm continuous spectrum) - was employed as a controllable light source. Software was written in C++ to control the photometer through a USB interface and for data acquisition. Pb(II) measurement is based on the AuNPs color change due to their aggregation provoked by Pb(II). The method showed excellent selectivity compared to other 19 metal ions ( $\text{Ag}^+$ ,  $\text{Al}^{3+}$ ,  $\text{Ba}^{2+}$ ,  $\text{Ca}^{2+}$ ,  $\text{Cd}^{2+}$ ,  $\text{Co}^{2+}$ ,  $\text{Cr}^{3+}$ ,  $\text{Cu}^{2+}$ ,  $\text{Fe}^{2+}$ ,  $\text{Hg}^+$ ,  $\text{K}^+$ ,  $\text{Li}^+$ ,  $\text{Mg}^{2+}$ ,  $\text{Mn}^{2+}$ ,  $\text{Na}^+$ ,  $\text{Ni}^{2+}$ ,  $\text{Sn}^{2+}$ ,  $\text{Sr}^{2+}$ , and  $\text{Zn}^{2+}$ ).  $\text{Pb}^{2+}$  was detected with the photometer and also monitored via UV-Vis. Solutions containing  $\text{Pb}^{2+}$  in the concentration range from 0.6 to 10  $\text{mmol L}^{-1}$  were employed to constructed the analytical curves, proving limits of detection (LOD) of 0.89  $\text{mmol L}^{-1}$ . The sensitivity was compared to those obtained with a UV-Vis spectrophotometer at 520 nm. A repeatability of 4.11 % (expressed as the relative standard deviation of 10 measurements) was obtained. The proposed method was successfully applied to detect  $\text{Pb}^{2+}$  in spiked water samples.

*Key-Words:* Photometer; sensor TCS230;  $\text{Pb}^{2+}$ ; Gold nanoparticles;

## Introduction

Many portable instruments have been made possible by the use of clever designs incorporating smaller components such as optical fibers,<sup>1</sup> light emitting diodes (LED),<sup>2</sup> liquid crystal displays (LCD),<sup>3</sup> and miniature gratings for use in spectrometers. The fact that these devices are smaller and lighter gives them the huge advantage of being easily transportable to the sample site to perform *in loco* measurements. Furthermore they take up less space in a laboratory, many of them can work off batteries, often cost less than conventional benchtop instruments, require less sample and reagents producing less waste, and are often simpler to use.<sup>4</sup>

Low-cost powerful microcontrollers are being included as control-processing units in many types of portable and hand-held instrumentation. One of the most popular open-source microcontroller is Arduino.<sup>5</sup> Arduino can be programmed with the measurement algorithms, calibration function, and drift corrections needed for the full instrument operation, with the numeric final result displayed on a screen. The Arduino platform has already found applications in analytical chemistry to construct a photometer portable for determination of Fe<sup>3+</sup> and Fe<sup>2+</sup> in fresh water<sup>6</sup> and the amount microorganisms in liquid culture.<sup>7</sup> Usually, the basic Arduino microcontroller (version “Uno”) comprises an ATmega chip that contains 14 digital inputs/outputs and 6 analogue inputs. It can be powered by battery or computer (via USB port). Finally, the scripts can be written in a language derived from C using free integrated development environment software and uploaded to the Arduino printed circuit board (PCB) via the USB port.

The recent advancements in the field of nanotechnology have opened up new arenas for the applications of nanomaterials including the development of ultrasensitive detection in the analytical sciences.<sup>8-10</sup> One potential approach is the use of noble metal

5

1  
2  
3 nanoparticles (e.g. gold and silver) as colorimetric probes.<sup>10,11</sup> Such a use relies on their  
4  
5 excellent and distinctive optical properties such as high visible-region extinction  
6  
7 coefficients and distance-dependent optical properties, which allow to visualize trace  
8  
9 level targets simply by the naked eye. For example, Huang and Chang developed a new  
10  
11 gold-nanoparticle based sensor for rapid determination of  $\text{Hg}^{2+}$  in aqueous  
12  
13 environmental samples and in batteries.<sup>12</sup> Li and Li<sup>13</sup> reported the development of a  
14  
15 highly sensitive and selective colorimetric detection method for cysteine using AuNPs.  
16  
17 This assay relies upon the distance-dependent optical properties of gold nanoparticles,  
18  
19 the self-assembly of cysteine on gold nanoparticles, and the interaction of a 2:1  
20  
21 cysteine/ $\text{Cu}^{2+}$  complex. In addition, the nanoparticles give high sensitivity for the  
22  
23 detection of metal ions due their optical properties exhibit shape,<sup>14</sup> strong size,<sup>15</sup> and  
24  
25 interparticle distance dependences.<sup>16</sup>  
26  
27  
28

29  
30 Lead is a non-ferrous metal widely used in batteries, paints, gasoline and  
31  
32 different alloys. Wastewater generated during the processing of lead-acid batteries  
33  
34 contains  $\text{Pb}^{2+}$ , which is very toxic to the environment and to living beings. Although  
35  
36 standard techniques such as atomic absorption spectroscopy (AAS),<sup>17</sup> anodic stripping  
37  
38 voltammetry,<sup>18</sup> inductively coupled plasma atomic emission spectroscopy (ICP-AES),<sup>19</sup>  
39  
40 or fluorescence spectrum<sup>20</sup> are efficient in determining  $\text{Pb}^{2+}$  levels in water, these  
41  
42 techniques are often costly, labor-intensive, time-consuming, require complex and  
43  
44 expensive instruments and specialized personnel to carry out the operational procedures.  
45  
46 For this reason there are ongoing researches on the development of rapid, low-cost and  
47  
48 friendly-use techniques suitable for *in situ* assays of heavy metals. In this paper, we  
49  
50 present a detailed explanation of the electronics of a home-made field-portable  
51  
52 photometer that accurately determines light absorbance. We tested the performance of  
53  
54 the photometer by measuring the amount of  $\text{Pb}^{2+}$  using AuNPs as colorimetric probes.  
55  
56  
57  
58  
59  
60

6

Since  $\text{Pb}^{2+}$  determination is relevant for studies involving aquatic environment, the instrument setup and the control software may be easily designed to carry out measurements *in loco*.

## Materials and methods

### Colorimetric LED photometer

#### Microcontroller

The instrument was based on an Arduino UNO plate. The Arduino UNO has a low cost (US\$ 24.95) and was programmed using the Arduino IDE 1.0.6 software. The general features of the Arduino's system are shown on Table 1.

[Insert Table 1 here]

#### Detector

A TCS230 was used as detector (Fig. 1a). It has 16 phototransistors for red filtering, 16 phototransistors for green filtering, 16 phototransistors for blue filtering, and 16 phototransistors without filtering (blank). Each phototransistor responds to their respective filtering color with an electrical signal proportional to the color intensity. This signal, which has a frequency proportional to the color intensity measured in each moment, is represented by a squared wave with a work cycle of 50% (Fig. 1c).

#### LED array

Four standard LEDs of 3.0 V and 20-25 mA with white color emission were used for irradiate the sample bucket. The LEDs were positioned on the four sides of the detector sensors (Fig. 1b).

7

[Insert Figure 1 here]

### Photometer overview

An LCD display JHD 162A was used to show the RGB intensity values to the user according to the detector output. Two potentiometers were used for controlling the light and the saturation on the LDC display. A resistor of 10 k $\Omega$  was used to control the current. The liquid sample is placed into a plastic bucket and positioned above the LED/detector system as can be seen in Fig. 2.

[Insert Figure 2 here]

The measure button (f1) starts the white LEDs and the detector at the same time. The RGB color values are shown on the LCD display during 20 seconds, until the system restarts. The button (f2) restarts the system.

### Data treatment

The RGB color intensity is provided directly by the TCS230 sensor. The Arduino code was adapted to normalize this value per 255 in order to decrease the range of signal value. After collecting the RGB intensity values from LCD display, a .TXT file was generated and loaded into MATLAB® R2012b (MathWorks, USA). The calibration was based on RGB intensity values according Eq. 1, in which the signal  $i$  behaves linearly with the concentration of AuNP with Pb(II).

$$i = g - b \quad (1)$$

where  $g$  and  $b$  are the GB (green and blue) intensity values shown on LCD display; and  $i$  is the intensity signal.



8

## Experimental procedure

### Synthesis and characterization of AuNPs

AuNPs were produced using a previously reported method<sup>20</sup> based on the reduction of Au<sup>3+</sup> with glycerol in alkaline medium. Briefly, all glassware was kept overnight in KMnO<sub>4</sub> + NaOH solution, rinsed with deionized water, kept for 10 min in H<sub>2</sub>O<sub>2</sub> + H<sub>2</sub>SO<sub>4</sub> solution (1:1 v/v), again rinsed with deionized water and dried prior to use. Afterwards, determined amounts of PVP (MW = 10.000) and gold chloride were dissolved in 10 ml of water. In a separate flask, fixed quantities of glycerol and NaOH were dissolved in 10 mL of water. The glycerol-NaOH solution was then added to the AuCl<sub>3</sub>-PVP solution to yield the following final concentrations: 1.0 mmol L<sup>-1</sup> Au<sup>3+</sup>, 0.10 mol L<sup>-1</sup> NaOH, 0.10 mol L<sup>-1</sup> glycerol and 10 g L<sup>-1</sup> PVP. The final mixture had a deep-red color due to the formed AuNPs. Finally, the AuNPs colloidal solution had then its pH adjusted to 7 by addition of diluted HCl. Considering a quantitative transformation of gold ions into nanoparticles, the concentration of AuNPs was estimated to be 8.0 x 10<sup>-8</sup> mol L<sup>-1</sup> based on their average size determined from TEM results.<sup>21</sup> UV-Vis absorption spectra of the AuNPs were acquired with an Evolution 60S UV-Visible spectrophotometer (Thermo Scientific) spectrophotometer. Transmission electron microscopy (TEM) images were acquired with a FEI Tecnai Spirit Biotwin 12 operating at 120 kV.

### Detection of Pb(II) by AuNPs

A Pb(NO<sub>3</sub>)<sub>2</sub> stock solution was prepared at the concentration of 20.0 mmol L<sup>-1</sup> from which different volumes were taken and then added to distinct aliquots of the AuNPs solution to yield Pb<sup>2+</sup> in the concentration range of 0.060 mmol L<sup>-1</sup> to 10.0 mmol L<sup>-1</sup>. In all cases the AuNPs concentration was kept at 2.0 x 10<sup>-8</sup> mol L<sup>-1</sup> by

9

1  
2  
3 adjusting the amount of water added to each mixture. The AuNPs-Pb<sup>2+</sup> solutions were  
4  
5 then analyzed by our colorimetric LED photometer with the RGB color intensity  
6  
7 directly recorded the TCS230 sensor. UV-Vis spectroscopy and TEM were also  
8  
9 conducted on the samples in order to acquire spectroscopic and morphology information  
10  
11 of the AuNPs, respectively, when in contact with Pb<sup>2+</sup>. The selectivity of the method  
12  
13 was investigated by performing experiments with the following salts: AgNO<sub>3</sub>,  
14  
15 AlCl<sub>3</sub>.6H<sub>2</sub>O, BaCl<sub>2</sub>.2H<sub>2</sub>O, CaCl<sub>2</sub>, CdCl<sub>2</sub>, CoCl<sub>2</sub>.6H<sub>2</sub>O, CrCl<sub>3</sub>.6H<sub>2</sub>O, CuSO<sub>4</sub>, FeCl-  
16  
17 2.4H<sub>2</sub>O, Hg<sub>2</sub>(NO<sub>3</sub>)<sub>2</sub>, KCl, LiCl, MgCl<sub>2</sub>.6H<sub>2</sub>O, MnCl<sub>2</sub>.4H<sub>2</sub>O, NaCl, NiCl<sub>2</sub>.6H<sub>2</sub>O,  
18  
19 SnCl<sub>2</sub>.2H<sub>2</sub>O, SrCl<sub>2</sub>.6H<sub>2</sub>O, Zn(CH<sub>3</sub>COO)<sub>2</sub>.2H<sub>2</sub>O.  
20  
21  
22

## 23 24 **Results and discussion**

### 25 26 27 **Mechanism of Pb(II) sensing by AuNPs**

28  
29  
30 Liu *et al.*<sup>22</sup> used glutathione-functionalized gold nanoparticles to colorimetrically  
31  
32 probe Pb<sup>2+</sup>. The authors argued that the -COOH and -NH<sub>2</sub> groups of glutathione could  
33  
34 bind to Pb<sup>2+</sup>, which provoked aggregation of gold nanoparticles with substantial shift in  
35  
36 the plasmon band energy to longer wavelength and a red-to-blue color change. In our  
37  
38 case PVP was used as stabilizer of AuNPs. PVP has an amide group that could in  
39  
40 principle chelate with Pb<sup>2+</sup> and, in addition, also concentrate Pb<sup>2+</sup> due to its shell-like  
41  
42 structure<sup>23</sup> around the particle. Chelating properties of PVP has been observed  
43  
44 elsewhere.<sup>24</sup> As shown by the UV-Vis and TEM results bellow, Pb<sup>2+</sup> was able to  
45  
46 promote size increase and aggregation of AuNPs, which is the base for Pb<sup>2+</sup> detection  
47  
48 with gold nanoparticles.  
49  
50  
51

52  
53 Fig. 3 shows a UV-Vis spectrum of the AuNPs produced by simple addition of  
54  
55 NaOH-glycerol to AuCl<sub>3</sub>-PVP at room temperature (red curve). Glycerol is an  
56  
57 inexpensive chemical and readily biodegradable under aerobic conditions, therefore an  
58  
59  
60

10

1  
2  
3  
4  
5  
6  
7  
8  
9  
10  
11  
12  
13  
14  
15  
16  
17  
18  
19  
20  
21  
22  
23  
24  
25  
26  
27  
28  
29  
30  
31  
32  
33  
34  
35  
36  
37  
38  
39  
40  
41  
42  
43  
44  
45  
46  
47  
48  
49  
50  
51  
52  
53  
54  
55  
56  
57  
58  
59  
60

eco-friendlier alternative compared to current reducing agents such as formamide, sodium borohydride and hydrazine. Visually the AuNPs solution is deep red, which is a consequence of the resonant coherent dipolar oscillations of the electron gas (electrons of the conduction band) at the surface of nanoparticles known as surface plasmon band (SPB). The colloidal AuNPs spectrum had a maximum absorbance ( $\lambda_{\text{Max}}$ ) at 520 nm, a value typical for spherical gold nanoparticles.<sup>20,25</sup> The symmetry of the band implies a fair similarity in the shape of the nanoparticles and low degree of aggregation in the solution.<sup>20</sup>

[Insert Figure 3 here]

The TEM image illustrated that the AuNPs (Fig. 4A) were well dispersed and spherical in shape, thus corroborating the UV-Vis results. The mean particle size calculated from the histogram of the inset of Fig. 4 was  $7.4 \text{ nm} \pm 2.8 \text{ nm}$ . Upon addition of  $0.10 \text{ mol L}^{-1} \text{ Pb}^{2+}$  the solution turned to a light violet due to aggregation stimulated by  $\text{Pb}^{2+}$ , which was confirmed by TEM (Fig. 4B) together with broadening and shifting of the peak to 590 nm in the UV-Vis spectrum (Fig. 3, blue curve)). The mean particle size is now  $8.9 \text{ nm} \pm 2.8 \text{ nm}$ . Another interesting feature of the AuNPs- $\text{Pb}^{2+}$  is the bimodal features of the particle size distribution (Fig. 4B), which is possibly due to ripening of big particles leading to the formation of extra small nanoparticles.<sup>20</sup>

[Insert Figure 4 here]

For the selectivity test AuNPs were exposed to  $0.10 \text{ mol L}^{-1}$  of the following metal ions:  $\text{Ag}^+$ ,  $\text{Al}^{3+}$ ,  $\text{Ba}^{2+}$ ,  $\text{Ca}^{2+}$ ,  $\text{Cd}^{2+}$ ,  $\text{Co}^{2+}$ ,  $\text{Cr}^{3+}$ ,  $\text{Cu}^{2+}$ ,  $\text{Fe}^{2+}$ ,  $\text{Hg}^+$ ,  $\text{K}^+$ ,  $\text{Li}^+$ ,  $\text{Mg}^{2+}$ ,  $\text{Mn}^{2+}$ ,  $\text{Na}^+$ ,  $\text{Ni}^{2+}$ ,  $\text{Sn}^{2+}$ ,  $\text{Sr}^{2+}$ , and  $\text{Zn}^{2+}$ . The UV-Vis spectra in Fig. 5 demonstrate qualitatively that those ions have no obvious impact on both SPB and color of AuNPs compared to  $\text{Pb}^{2+}$ , which suggests that the method is specific to  $\text{Pb}^{2+}$ .

11

[Insert Figure 5 here]

The selectivity of the method can be quantitatively assessed by factor  $F$  calculated for each metal ion according to Eq. 2:

$$F = 1 - \frac{A_{520}}{A^0_{520}} \quad (2)$$

where  $A_{520}$  is the absorbance at 520 nm of the AuNPs when exposed to a given metal ion and  $A^0_{520}$  is the absorbance at 520 nm of the pure AuNPs. An  $F$  value far from the unity signifies that a given metal ion had little impact on the SPB of the AuNPs. As can be seen in Fig. 6 all the ion metals except  $\text{Pb}^{2+}$  generated  $F$  values that strongly departed from the unity, which proves that the method is quite selective to  $\text{Pb}^{2+}$ .

[Insert Figure 6 here]

### Photometer results

Analytical curves were obtained for  $\text{Pb}^{2+}$  in spiked water samples using the developed photometer analyzed at five  $\text{Pb}^{2+}$  concentration levels, which show an excellent adjustment ( $r^2 = 0.995$ ) and a measurement range from 0.6 to 10.0 mmol L<sup>-1</sup>, as shown in Fig. 7. Once the signals from the LED for  $\text{Pb}^{2+}$  samples with AuNPs were registered by the photometer, the samples were immediately inserted into the other transmission cell coupled to the spectrophotometer for the registration of trade spectra (also Fig. 7). As shown in Fig. 7, the linearity of the calibration curve for  $\text{Pb}^{2+}$  was confirmed by the low lack of fit according to the experimental  $F$  value of 0.0429.<sup>26,27</sup> Comparing the sensitivities between the two instruments, it can be concluded that the

12

1  
2  
3 sensitivities were quite similar (0.171 and 0.161 for UV-Vis and photometer responses,  
4 respectively). The precision obtained for the photometer was studied at three  
5 concentration levels, namely 1 mmol L<sup>-1</sup>, 2 mmol L<sup>-1</sup>, and 10 mmol L<sup>-1</sup>, using 9  
6 different samples obtaining relative standard deviations between 5.50 % and 8.26 %  
7 when expressed as Pb<sup>2+</sup> concentration. In addition, the LOD for Pb<sup>2+</sup> photometer was  
8 0.89 mmol L<sup>-1</sup> and the limit of quantification (LOQ) was 2.69 mmol L<sup>-1</sup>, as calculated  
9 from modern IUPAC recommendation.<sup>27</sup>  
10  
11

12  
13  
14  
15  
16  
17  
18  
19 The fact that LOD and LOC were relatively high compared to the literature<sup>28,29</sup>  
20 may be explained as follows: i) PVP is a long polymer that involves the nanoparticles  
21 forming a shell-like structure,<sup>30</sup> thus high concentration of Pb<sup>2+</sup> is required for it to  
22 reach the AuNPs surface, disrupt the PVP protective layer, and promote AuNPs  
23 aggregation. Usually noble nanoparticles are produced with sodium citrate or sodium  
24 borohydride and anion adsorption confers the nanoparticle a negative charge that  
25 prevents aggregation through simple coulombic repulsion. As the citrate and  
26 borohydride anions are much smaller than PVP, the nanoparticle surface is naturally  
27 more accessible to heavy metals and lower concentrations may be used; ii) some works  
28 in the literature have achieved low detection limits by attaching specific recognition  
29 units such as DNA<sup>28,29</sup> and enzymes<sup>31</sup> to the nanoparticle surface, however the  
30 functionalization is complex and expensive. Furthermore the stability of the DNA poses  
31 problems for application in real samples. In this work we used an extremely-simple  
32 environmentally-correct route to produce stable AuNPs using glycerol and PVP as  
33 reducing and protective agents, respectively. We sought to present a home-made  
34 equipment that could be used for a relevant application, and a comparison with UV-vis  
35 results showed success in this matter.  
36  
37  
38  
39  
40  
41  
42  
43  
44  
45  
46  
47  
48  
49  
50  
51  
52  
53  
54  
55  
56  
57  
58  
59  
60

[Insert Figure 7 here]

## Conclusion

A novel photometer for  $\text{Pb}^{2+}$  detection using AuNPs as signal producer has been successfully developed. The photometer based on sensor TCS230 and an Arduino electronic card as acquisition system was a simple and low-cost assembly. These features may enable the proposed approach to be used as a stand-alone setup for  $\text{Pb}^{2+}$  determination in water. In addition, we believe that this approach may serve as a foundation for the preparation of practical nanosensors for the rapid determination of  $\text{Pb}^{2+}$  concentrations in aqueous samples, having the features required to become a field instrument.

## Acknowledgements

The authors would like to acknowledge the financial support from the CNPq for a fellowship for Morais, C.L.M, the Graduate Program in Chemistry of UFRN. The work was funded by grants from CNPq/Capes project (Grants 070/2012 and 442087/2014-4) and FAPERN (Grant 004/2012).

## References

- 1 F. Antonucci, F. Pallottino, G. Paglia, A. Palma, S. D'Aquino and P. Menesatti, *Food Bioprocess Technol.*, 2010, **4**, 809–813.
- 2 K. M. G. de Lima, *Microchem. J.*, 2012, **103**, 62–67.
- 3 E. S. Rich and J. E. Wampler, *Instrum. Sci. Technol.*, 1982, **12**, 65–74.
- 4 E. D. N. Gaião, S. R. B. dos Santos, V. B. dos Santos, E. C. L. do Nascimento, R. S. Lima and M. C. U. de Araújo, *Talanta*, 2008, **75**, 792–796.
- 5.

14

- 1  
2  
3  
4  
5  
6  
7  
8  
9  
10  
11  
12  
13  
14  
15  
16  
17  
18  
19  
20  
21  
22  
23  
24  
25  
26  
27  
28  
29  
30  
31  
32  
33  
34  
35  
36  
37  
38  
39  
40  
41  
42  
43  
44  
45  
46  
47  
48  
49  
50  
51  
52  
53  
54  
55  
56  
57  
58  
59  
60
- 6 J. C. Miranda, M. Y. Kamogawa and B. F. Reis, *Sensors Actuators B. Chem.*, 2015, **207**, 811–818.
- 7 J. J. Lamb, J. J. Eaton-Rye and M. F. Hohmann-Marriott, *Curr. Microbiol.*, 2013, **67**, 123–9.
- 8 B.-C. Ye and B.-C. Yin, *Angew. Chem. Int. Ed. Engl.*, 2008, **47**, 8386–9.
- 9 Y. Hung, T. Hsiung, Y. Chen and Y. Huang, *J. Phys. Chem. C*, 2010, **114**, 16329–16334.
- 10 G. K. Darbha, A. K. Singh, U. S. Rai, E. Yu, H. Yu and P. Chandra Ray, *J. Am. Chem. Soc.*, 2008, **130**, 8038–43.
- 11 H. Li, Q. Zheng and C. Han, *Analyst*, 2010, **135**, 1360–4.
- 12 C. Huang and H. Chang, *Anal. Chem.*, 2006, **78**, 8332–8338.
- 13 L. Li and B. Li, *Analyst*, 2009, **134**, 1361–5.
- 14 Y. Sun and Y. Xia, *Science (80-. )*, 2002, **298**, 2176–2179.
- 15 W. Haiss, N. T. K. Thanh, J. Aveyard and D. G. Fernig, *Anal. Chem.*, 2007, **79**, 4215–4221.
- 16 N. Malikova, I. Pastoriza-santos, M. Schierhorn, N. A. Kotov and L. M. Lizmarza, *Langmuir*, 2002, **18**, 3694–3697.
- 17 M. Ghaedi, F. Ahmadi and A. Shokrollahi, *J. Hazard. Mater.*, 2007, **142**, 272–8.
- 18 Y. Bonfil and E. Kirowa-Eisner, *Anal. Chim. Acta*, 2002, **457**, 285–296.
- 19 K. S. Rao, T. Balaji, T. P. Rao, Y. Babu and G. R. K. Naidu, 2002, **57**, 1333–1338.
- 20 J. J. Peterson and T. D. Krauss, *Nano Lett.*, 2006, **6**, 510–4.
- 21 X. Liu, M. Atwater, J. Wang, Q. Huo, *Colloids Surf. B Biointerfaces*, 2007, **58**, 3–7.
- 22 J. Liu and Y. Lu, *J. Am. Chem. Soc.*, 2003, **125**, 6642–6643.
- 23 Z. Wang, J. H. Lee and Y. Lu, *Adv. Mater.*, 2008, **20**, 3263–3267.
- 24 M. Su, C. Bai and C. Wang, *Solid State Commun.*, 1998, **106**, 643–645.
- 25 C. W. Lien, Y. T. Tseng, C. C. Huang and H. T. Chang, *Anal. Chem.*, 2014, **86**, 2065–2072.
- 26 K. Danzer and L. A. Currie, *Pure Appl. Chem.*, 1998, **70**, 993–1014.

15

- 1  
2  
3 27 A. C. Olivieri, *Anal. Chim. Acta*, 2015, **868**, 10–22.  
4  
5 28 J. Liu, Y. Lu, *J. Am. Chem. Soc.* 2003, **125**, 6642–6643.  
6  
7 29 Z. Wang, J.H. Lee, Y. Lu, *Adv. Mater.* 2008, **20**, 3263–3267.  
8  
9 30 M. Su, C. Bai, C. Wang, *Solid State Commol L-1 un.* 1998, **106**, 643–645.  
10  
11 31 C.W. Lien, Y.T. Tseng, C.C. Huang, H.T. Chang, *Anal. Chem.* 2014, **86**, 2065–  
12 2072.  
13  
14  
15  
16  
17  
18  
19  
20  
21  
22  
23  
24  
25  
26  
27  
28  
29  
30  
31  
32  
33  
34  
35  
36  
37  
38  
39  
40  
41  
42  
43  
44  
45  
46  
47  
48  
49  
50  
51  
52  
53  
54  
55  
56  
57  
58  
59  
60



16

**Legends to Figures**

**Figure 1:** Functional block diagram of the Arduino TCS230 color recognition sensor module. (a) TCS230 sensor; (b) photodiode array; (c) current to frequency converter.

**Figure 2:** Overview of RGB photometer: (a) LED Array with sensor; (b) power supply and USB interface for data acquisition; (c) Arduino microcontroller for powering the sensor; (d) homemade cell; (e) display; (f1) and (f2) controller buttons.

**Figure 3:** UV-vis spectra of AuNPs in absence and presence of 0.1 M  $\text{Pb}^{2+}$ .

**Figure 4:** TEM of AuNPs in (A) absence and (B) presence of 0.1 M  $\text{Pb}^{2+}$ .

**Figure 5:** UV-Vis absorption spectra of AuNPs in presence of 0.1 M metal ions: (–) AuNPs pure; (–) AuNPs + 19 metal ions; (–) AuNPs +  $\text{Pb}^{2+}$ .

**Figure 6:** Selectivity factor for 20 metal ions exposed to AuNPs.

**Figure 7:** Analytical curves for a series of standard  $\text{Pb}^{2+}$  solutions complexed with AuNP in two instruments: (a) RGB photometer data are represented with blue circles; (b) Thermo scientific 60S UV-Vis spectrophotometer data are represented with green triangles, at  $\lambda = 520$  nm. All measurements are made in a 1 cm path cell.

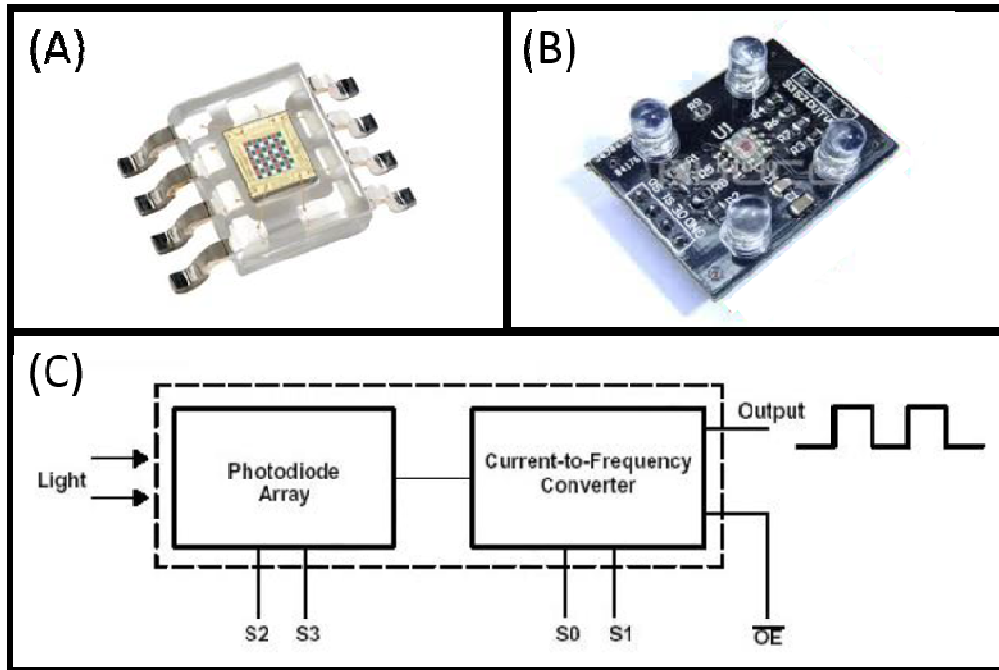
**Legends to Tables**

**Table 1.** Arduino UNO features of the colorimetric LED photometer.

17

Figures

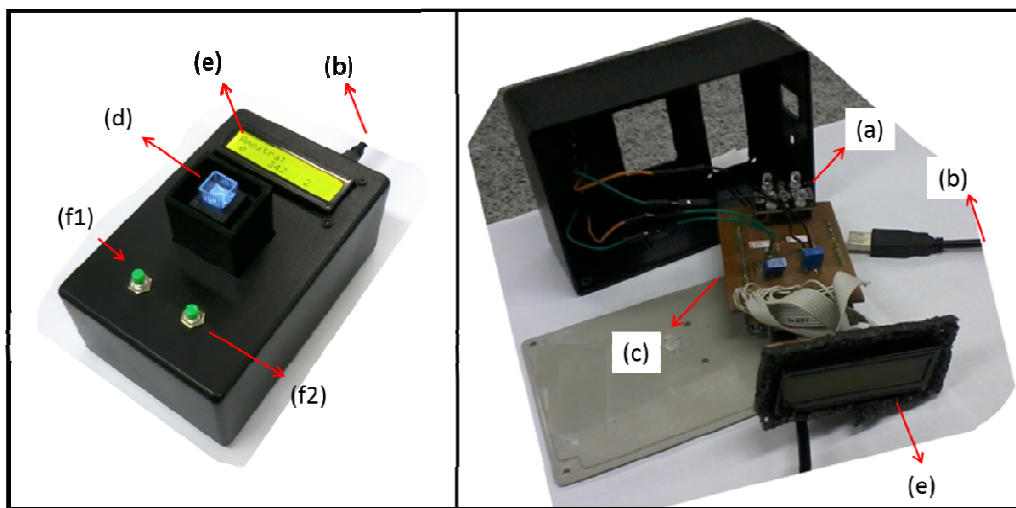
Figure 1



1  
2  
3  
4  
5  
6  
7  
8  
9  
10  
11  
12  
13  
14  
15  
16  
17  
18  
19  
20  
21  
22  
23  
24  
25  
26  
27  
28  
29  
30  
31  
32  
33  
34  
35  
36  
37  
38  
39  
40  
41  
42  
43  
44  
45  
46  
47  
48  
49  
50  
51  
52  
53  
54  
55  
56  
57  
58  
59  
60

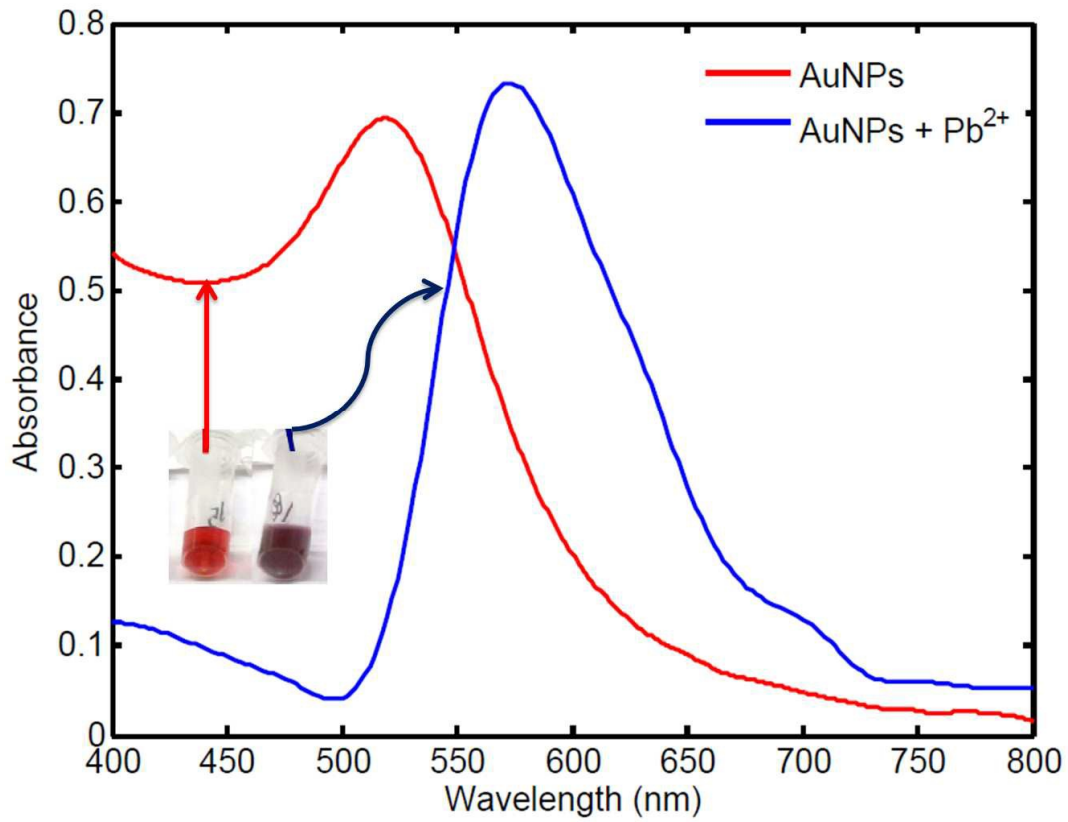
18

Figure 2

1  
2  
3  
4  
5  
6  
7  
8  
9  
10  
11  
12  
13  
14  
15  
16  
17  
18  
19  
20  
21  
22  
23  
24  
25  
26  
27  
28  
29  
30  
31  
32  
33  
34  
35  
36  
37  
38  
39  
40  
41  
42  
43  
44  
45  
46  
47  
48  
49  
50  
51  
52  
53  
54  
55  
56  
57  
58  
59  
60

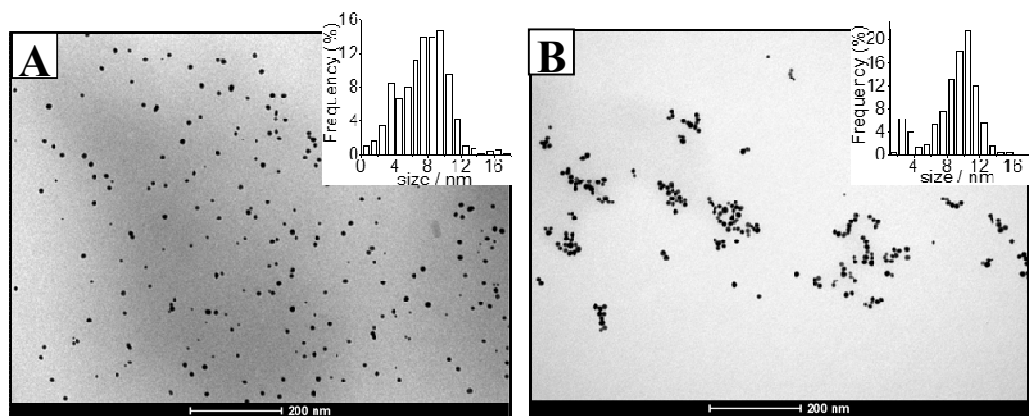
19

Figure 3



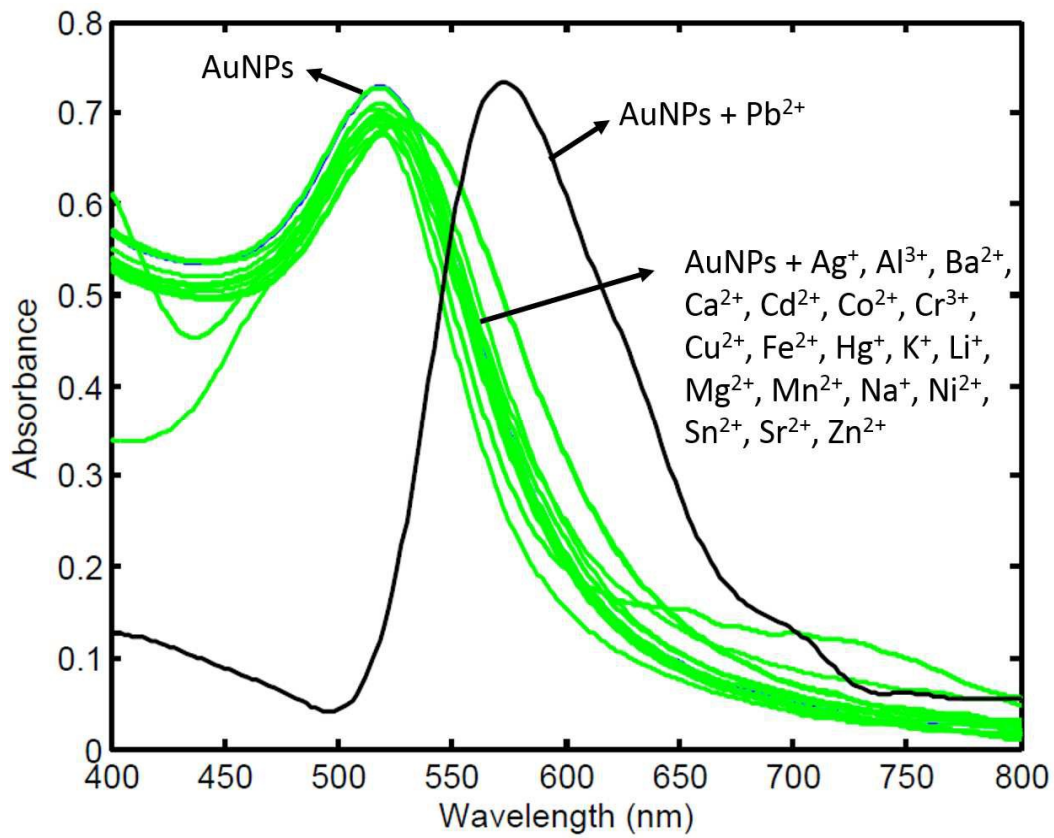
20

Figure 4

1  
2  
3  
4  
5  
6  
7  
8  
9  
10  
11  
12  
13  
14  
15  
16  
17  
18  
19  
20  
21  
22  
23  
24  
25  
26  
27  
28  
29  
30  
31  
32  
33  
34  
35  
36  
37  
38  
39  
40  
41  
42  
43  
44  
45  
46  
47  
48  
49  
50  
51  
52  
53  
54  
55  
56  
57  
58  
59  
60

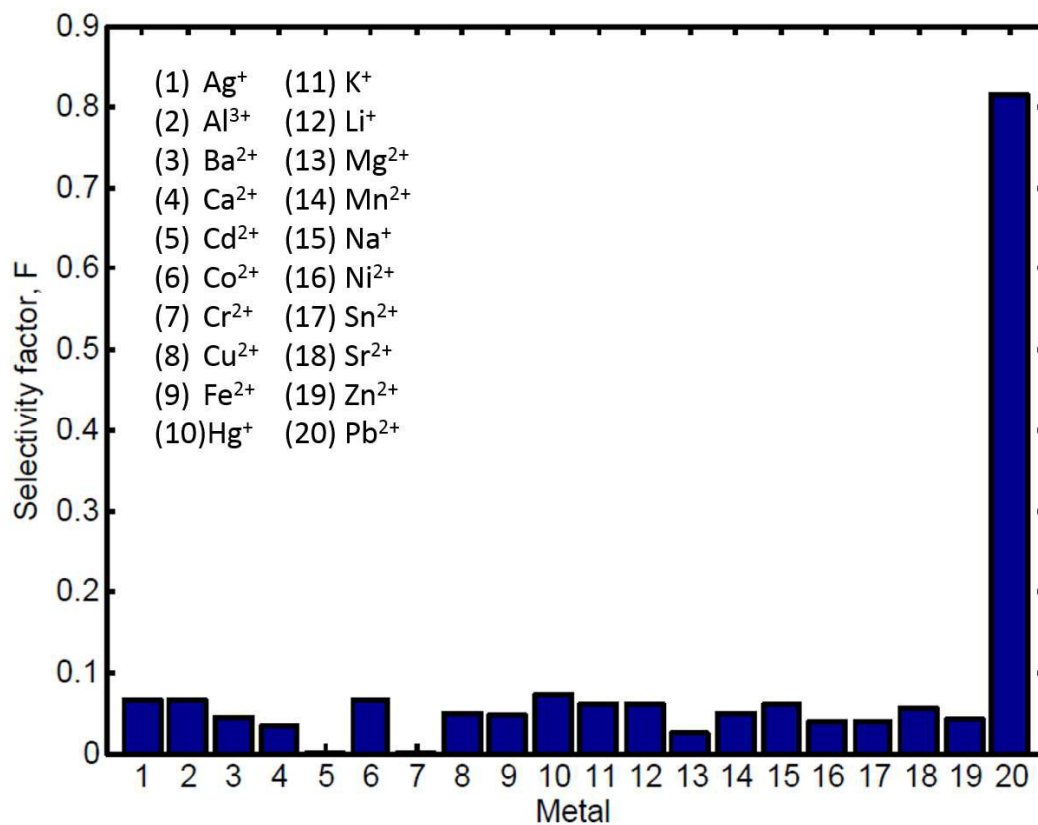
21

Figure 5



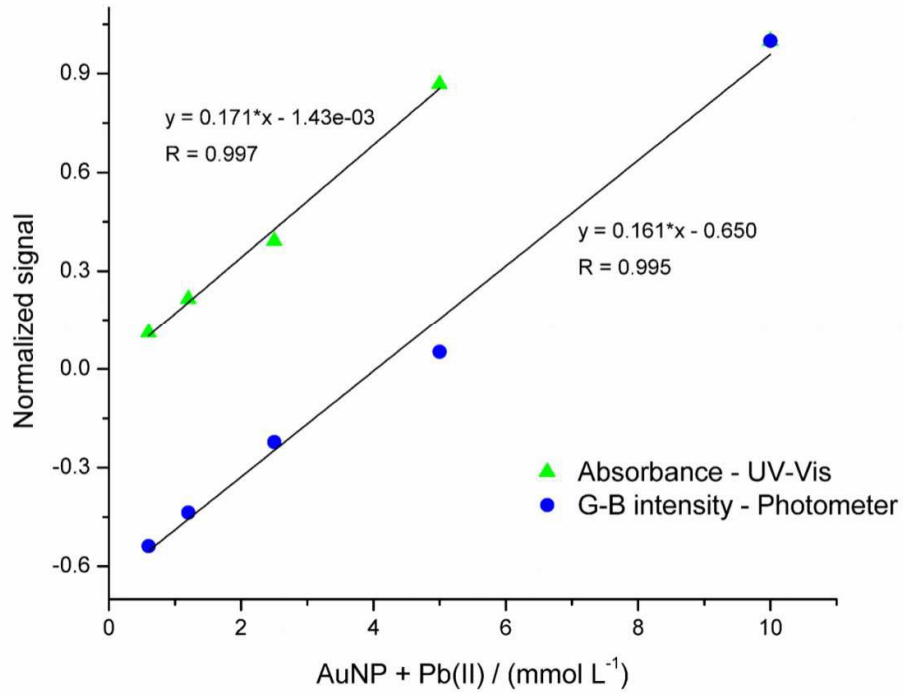
22

Figure 6



23

Figure 7





24

**Tables****Table 1**

Microcontroller chip	ATmega328
Working tension	5 V
Input tension (recommol L-1 ended)	7 – 12 V
Digital I/O pin	14
Analogical I/O pin	6
DC current per I/O pin	40 mA
Flash memory	32 KB
SRAM memory	2 KB
EEPROM memory	1 KB
Clock speed	16 MHz